Century-Scale Intensity Modulation of Large-Scale Variability in Long Historical Temperature Records

NAIMING YUAN

Laboratory for Climate and Ocean–Atmospheric Studies, Department of Atmospheric and Oceanic Science, School of Physics, Peking University, and Chinese Academy of Meteorological Science, Beijing, China

ZUNTAO FU

Laboratory for Climate and Ocean–Atmospheric Studies, Department of Atmospheric and Oceanic Science, School of Physics, Peking University, Beijing, China

(Manuscript received 18 June 2013, in final form 23 October 2013)

ABSTRACT

Large-scale variability in long historical temperature records around the North Atlantic Ocean is analyzed by means of power spectral density (PSD) analysis and detrended fluctuation analysis (DFA). It is found that the intensity of large-scale variability is changeable with time, and long memory analysis can be used to detect this possible intensity variation quantitatively. By estimating long-term memory (LTM) in subrecords of different time intervals, a century-scale variation of LTM is revealed, which further indicates a century-scale intensity modulation of the large-scale temperature variability. At the beginning of the nineteenth and twentieth centuries, the large-scale variability is more apparent, whereas in the second half of the nineteenth and twentieth centuries the large-scale variability becomes less significant. Considering the importance of large-scale variability, the findings herein suggest a new perspective on the understanding of climatic change.

1. Introduction

It is well recognized that the global climate over the past centuries exhibits substantial variability on time scales of a century or less (Schlesinger and Ramankutty 1994; Mann et al. 1995; Becker et al. 1999). Especially in the North Atlantic, the well-known Atlantic multidecadal oscillation (AMO), which may be driven by the ocean's thermohaline circulation, is particularly notable and has been thought responsible for the observed variations in nearby regions (Delworth and Mann 2000; Gray et al. 2004; Sutton and Hodson 2005). In light of this large-scale/low-frequency variability (LFV), one can better predict climate or, more essentially, gain in-depth understanding of the mechanisms of climate change (Mann et al. 1998; Keenlyside et al. 2008; Ottera et al. 2010; Franzke and Woollings 2011). Therefore, it is of great importance to study the large-scale climate variability systematically, as many scientists have already done during the past few decades (Marshall et al. 2001; Dima and Lohmann 2004; Grosfeld et al. 2007).

However, when studying the large-scale climate variability, in addition to the time scales on which the climate may vary, one also needs to know whether, or in what pattern, the intensity of the large-scale variability changes with time. Even though, because of the time limits of our instrumental data, it is not easy to implement rigid research for multidecadal scales, for shorter scales (from 3 months to 3 yr) we still may find some hints for the possible changing intensity. To detect these hints is thus the main focal point of this study.

A traditional method we can use to describe how a time series oscillates on different time scales is the so-called power spectral density (PSD) analysis. In a climatic time series, it is normal to get high power at low frequency and low power at high frequency (Hasselmann 1976), as shown by Fig. 1b. Since higher power at low frequency normally indicates more apparent large-scale variability, by comparing the PSD calculated from different time intervals, one can determine whether there is an intensity

Corresponding author address: Zuntao Fu, Laboratory for Climate and Ocean–Atmosphere Studies, Dept. of Atmospheric and Oceanic Sciences, School of Physics, Peking University, Beijing, 100871, China.
E-mail: fuzt@pku.edu.cn

DOI: 10.1175/JCLI-D-13-00349.1

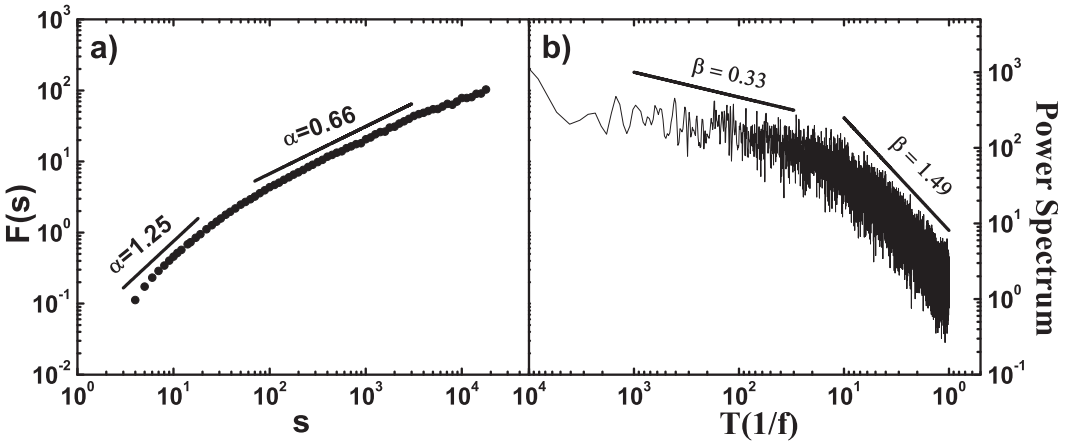

FIG. 1. Results of (a) DFA-2 and (b) power spectral analysis for the daily-mean temperature records in Milan. For different time scales, the DFA-2 exponent α in (a) and the power spectrum exponent β in (b) are different. For larger scale ($\geq$100 days), $\alpha = 0.66$ and $\beta \approx 0.33$, whereas for smaller scales ($\leq$20 days), $\alpha = 1.25$ and $\beta \approx 1.49$. Values of α and β obtained in the figure comply with the relationship $\alpha = (1 + \beta)/2$, which means that over a large-scale range, the stronger the LTM is, the more apparent large-scale variability might be.

variation of climate variability at large time scales, as shown in Fig. 2a. However, it is difficult to determine the variation quantitatively given the poor statistics of PSD on large time scales, so we employ another well-developed method, detrended fluctuation analysis (DFA) (Peng et al. 1994; Kantelhardt et al. 2001). In DFA, the fluctuation function $F(s)$ is used, which is calculated from a given time series on different time scales of s, to represent the variabilities. It is proved that $F(s)$ obtained from DFA has a close relationship with PSD, but it is less influenced by the statistical uncertainty resulting from the multiwindow detrending and averaging procedure (Talkner and Weber 2000), as shown in Fig. 1. Therefore, we can use the results of DFA as a better measurement of the climate variability. For more details of DFA, please refer to section 2.

Actually, DFA is mainly applied for the estimation of the well-known phenomenon of long-term memory (LTM) (Koscielny-Bunde et al. 1998; Fraedrich and Blender 2003; Rybski et al. 2006; Chen et al. 2007; Vyushin and Kushner 2008; Mann 2011). When a given time series is long-term correlated, its result normally exhibits a power-law scaling behavior [$F(s) \sim s^{\alpha}$] and its autocorrelation function $C(s)$ decays slowly also as a power law [$C(s) \sim s^{-\gamma}$] (Kantelhardt et al. 2001), which indicates self-similarity. Since the stronger the LTM is, the more apparent large-scale variability might be (Zhu et al. 2010), it follows that by analyzing whether the LTM varies with time, one can show if, or in what pattern, the intensity of the large-scale variability varies with time. Therefore, our concern in this study can also be considered as a detection of the LTM variation.

In view of the well-known AMO and its influence on climate in nearby regions, here we use 12 instrumentally long temperature records observed around the North Atlantic Ocean for analysis. By determining the LTM of subrecords from different time intervals, a century-scale variation cycle is found, which may indicate a possible intensity variation of the climate large-scale variability, and lead to a new perspective on climate change.

2. Data and methodology

a. Data

The 12 daily long-term temperature records are obtained from the Royal Netherlands Meteorological Institute (KNMI) Climate Explorer (http://climexp.knmi.nl/). Details are shown in Table 1. We use these 12 temperature records for our research because of two considerations: 1) The records are all observed around the North Atlantic Ocean. 2) They all have long history with few missing points. Some records' length can be even longer than 200 years. It is worth noting that we use the minimum temperature for two stations (Toronto and Rhein-Main), unlike for other stations for which the mean temperature records are our main research objects. This is because we do not have the mean temperature data for these two stations. From the results, however, we can see little difference between the mean and the minimum temperature (see Fig. 4, the results of Prague and Vienna). Therefore, these two stations with only minimum temperatures are included in our study.

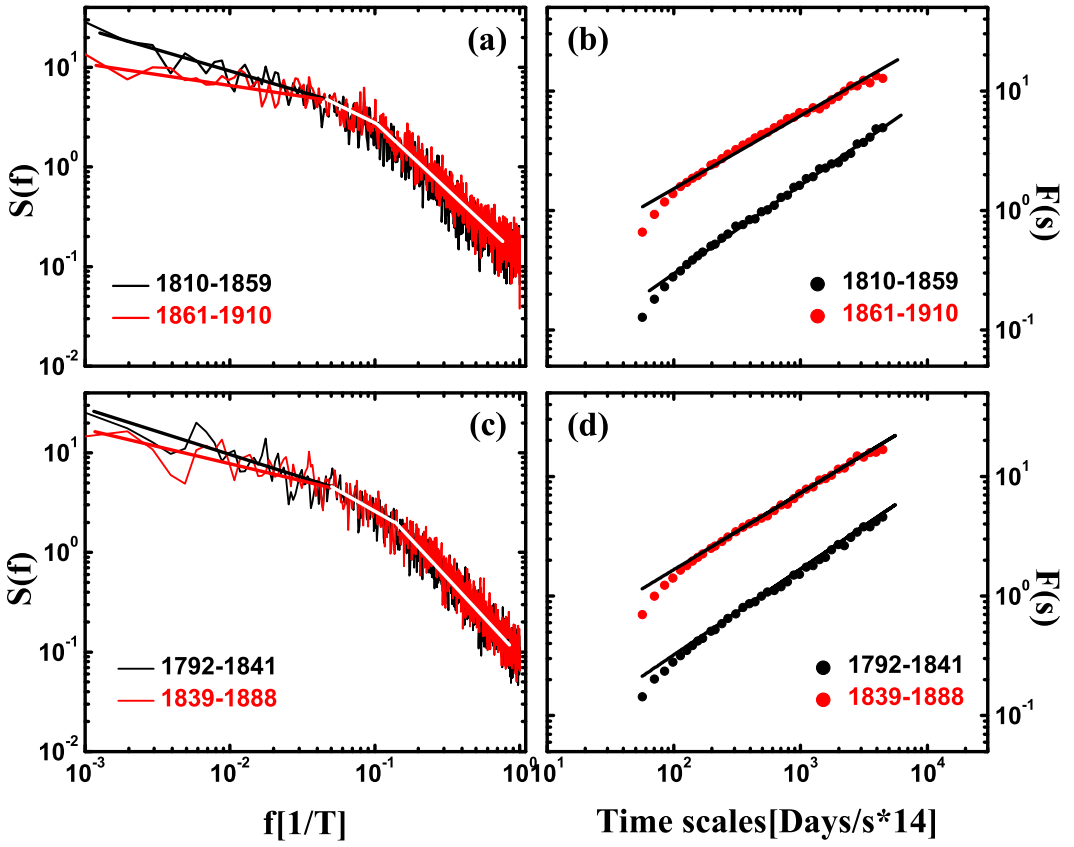

FIG. 2. Results of (a),(c) power spectral analysis and (b),(d) DFA-2 of subrecords from two different time intervals, for (top) Milan and (bottom) Prague (maximum temperature). It can be seen that remarkable differences arise over large-scale range (≥100 days), which indicates an intensity variation of the large-scale variability.

Before our analysis, we first standardize the data by (i) averaging the daily data over 2-week-long nonoverlapping windows to remove the short-term correlations resulting from general weather regimes and (ii) removing the seasonal trend through subtracting the annual cycle, as $\tau_i = T_i - \langle T_i \rangle$ (Koscielny-Bunde et al. 1998), where T_i is the biweekly temperature and τ_i the temperature anomalies that we use for analysis. Considering the possible changes of annual cycle over the past few centuries, we employ a sliding-window method for calculation. We take 31 yr as the size of the window, and calculate the annual cycle in each window. The annual cycle determined is then subtracted by the mid-year (or the 16th year in each window). In this way, 30 yr of data (15 yr at the beginning and another 15 yr at the end of the record) will not be taken into account. For example, we only consider the temperature anomalies from 1778 to 1992 (215 yr) in Milan.

TABLE 1. Details of the data we use for analysis.

Station	Country	Location (lat, lon)	Max/min/mean temperature records	Dates	Length (yr)
Milan	Italy	45.47°N, 9.19°E	Mean	1763–2007	245
Prague	Czech Republic	50.09°N, 14.42°E	Max,min,and mean	1775–2004	230
Hohenpeissenburg	Germany	47.80°N, 11.01°E	Mean	1781–2011	231
Bologna	Italy	44.50°N, 11.35°E	Mean	1814–2011	198
Toronto	Canada	43.67°N, 79.40°W	Min	1841–2002	162
Vienna	Austria	48.23°N, 16.35°E	Max, min, and mean	1856–2011	156
Zagreb-Gric	Croatia	45.82°N, 15.98°E	Mean	1862–2011	150
Rhein-Main	Germany	50.03°N, 8.58°E	Min	1870–2011	142

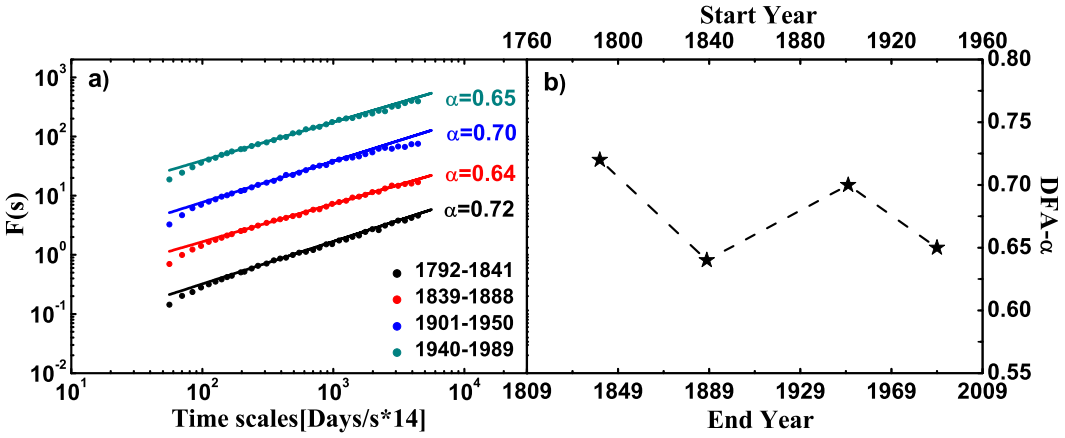

FIG. 3. (a) DFA-2 results of the subrecords (50 yr) extracted from the biweekly mean temperature data of Prague. Different LTMs are obtained in different time windows. In the time windows of 1792–1841 (black), $\alpha = 0.72$; 1839–88 (red), $\alpha = 0.64$; 1901–50 (blue), $\alpha = 0.70$; and 1940–89 (green), $\alpha = 0.65$. (b) The variation of α values with time. Numbers on the top of the figure are the start year for each time window, while at the bottom of the figure are the end year of the corresponding time window.

b. Methodology

For analyzing the LTM in a given dataset, we employ the detrended fluctuation analysis of second order (DFA-2) (Kantelhardt et al. 2001). In DFA-2, one usually does not calculate the variance of the record of interest $\{x_j\}$ directly, but considers the cumulated sum (profile) $Y_i = \sum_{j=1}^{i} x_j$. One divides the profile into nonoverlapping segments of size s. In each segment ν, the best quadratic fit of the profile and the standard deviation of the profile around this fit are determined. Then we average the result over all windows ν to obtain the mean fluctuation function $F(s)$. One is interested in the dependence of $F(s)$ on s. For the case of LTM, $F(s)$ increases by a power law $F(s) \sim s^{\alpha}$, with the exponent $\alpha > 0.5$. Meanwhile, the power spectral density $S(f)$ also decays as a power law $S(f) \sim f^{-\beta}$, and the exponent β has a relationship with α as $\alpha = (1 + \beta)/2$ (Kantelhardt et al. 2001). As shown in Fig. 1, high α corresponds to high β, and vice versa. Therefore, on large scales, a stronger LTM (high α) normally means more apparent large-scale variability (high β), which further indicates high predictability of the climate (Zhu et al. 2010).

To determine whether the LTM varies with time, we extract subrecords according to a 50-yr sliding window in each standardized data. For example, 166 subrecords can be extracted from Milan (215 yr; 1778–1992), namely 1778–1827, 1779–1828, ... , 1943–92. By determining the LTM in each subrecord within the scaling range from 100 to 1000 days (or roughly from 3 months to 3 yr), we can find whether the LTM, or the intensity of the large-scale variability, varies with time.

3. Results

Before our analysis, we first employ DFA-2 to these 12 temperature records and find that all the α values are larger than 0.5 (ranging from 0.6 to 0.7; not shown here). This means all the records are long-term correlated, and the α values obtained are in line with previous findings (Koscielny-Bunde et al. 1998). However, according to the procedures of DFA, the fluctuation function $F(s)$ is averaged over all the time periods. For detailed information, a further analysis on the subrecords from different time intervals is needed.

As shown in Fig. 2, we take the mean temperature in Milan and the maximum temperature in Prague as examples. One can find that in different time intervals, the scaling behaviors can be remarkably different over large-scale range (100–1000 days), which further indicates an intensity variation of the large-scale variability, as shown in Figs. 2a and 2c. Since the power spectral density fluctuates tremendously at large scale (Figs. 2a,c), we prefer to use the results of DFA as a better measurement of the climate variability (Figs. 2b,d). In Fig. 3, we randomly select four time periods in Prague for analysis. Interestingly, in the time window of 1792–1841, a relatively stronger LTM ($\alpha = 0.72$) is found, while in the following window of 1839–88, the correlations become weaker ($\alpha = 0.64$). For the twentieth century, the LTM again becomes stronger in the first half (time window of 1901–50, $\alpha = 0.70$), and then weaker (time window of 1940–89, $\alpha = 0.65$). There seems to be a quasi-century variation cycle, as shown in Fig. 3b.

However, we note that this variation cycle needs to be confirmed very carefully. As some former works

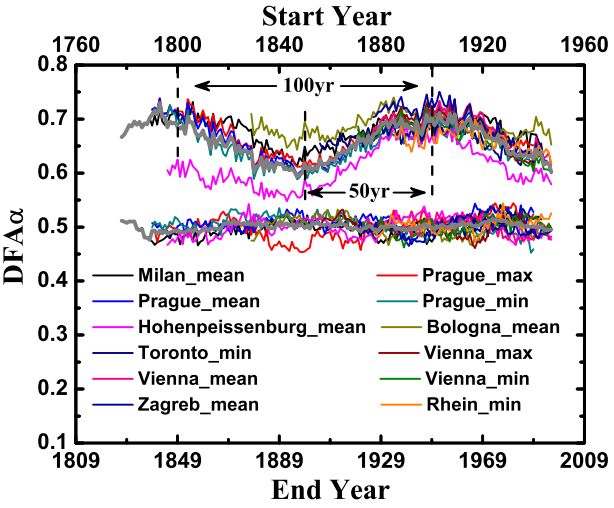

FIG. 4. Variation of α values obtained by DFA-2, for 1) all of the 12 long temperature records (top curves) and 2) the shuffled records derived from the 12 long temperature records (bottom curves). By averaging the results over the 12 samples, we can obtain an average curve, which is shown as the thick gray line. There is a remarkable century-scale oscillation of LTM in the long historical temperature records, whereas for the shuffled records the average line is flat. As in Fig. 3b, numbers at the top (bottom) of the figure are the start year (end year) of each time window.

discussed (e.g., Rybski and Bunde 2009; Lennartz and Bunde 2009), for a long time series with a given DFA exponent α, if we divide the data into many short subrecords, the α values of the subrecords may vary tremendously for statistical reasons, and $F(s)$ values averaged over different time intervals can be different only as a result of statistical uncertainty. Therefore, to make sure whether the quasi-century variation cycle shown in Fig. 3 is induced by intrinsic property, we further made the same analysis to 1) all the 12 long-term temperature records and 2) shuffled records derived from the 12 temperature records. Figure 4 shows the results, according to which we argue that the LTM does have a century-scale cycle signal. There are two pieces of evidence, as follows:

1) For all the 12 temperature records, as shown in Fig. 4, the α values (obtained from subrecords with a scaling range of 100–1000 days) vary with time according to a similar pattern. They all have relatively higher α at the beginning of the nineteenth and twentieth centuries and lower α around the second half of the nineteenth and twentieth centuries. By further averaging the results over the 12 samples (see the gray thick line shown in Fig. 4) a clear century-scale variation is obtained. If the variation of α is only a result of statistical uncertainty, it is unlikely that all the 12 temperature records would have one similar pattern. In other words, there should be a dynamic mechanism that governs the variation of LTM.
2) After the 12 temperature records are shuffled (LTM is removed), as shown in Fig. 4, although variations of α still arise, the shuffled records have random phases (or patterns), which therefore result in a "flat-average line" (the gray thick line in Fig. 4). This means the method itself will not result in any "cycle signal" and is reliable for detection.

To better illustrate the results shown in Fig. 4, Table 2 shows the statistical properties of the α values. It is easy to find that the standard deviations, or the range of the α variations obtained from the 12 temperature records, are all larger than that obtained from the shuffled data. Since the α variations obtained from the shuffled data should result from the statistical uncertainty and the

TABLE 2. Statistical properties of the α values in Fig. 4, including the standard deviation, maximum, minimum, and the range of the α variation. The bottom row shows the results of the averaged α variation (over the 12 samples).

Station	Temperature record	From temperature records				From shuffled data			
		Std dev	Max	Min	Range	Std dev	Max	Min	Range
Milan	Mean	0.026	0.73	0.61	0.12	0.017	0.54	0.47	0.07
Prague	Max	0.034	0.74	0.61	0.13	0.022	0.54	0.45	0.09
	Mean	0.036	0.74	0.60	0.14	0.015	0.54	0.47	0.07
	Min	0.033	0.73	0.59	0.14	0.015	0.53	0.45	0.08
Hohenpeissenburg	Mean	0.038	0.69	0.55	0.14	0.018	0.54	0.47	0.07
Bologna	Mean	0.022	0.74	0.64	0.10	0.015	0.53	0.47	0.06
Toronto	Min	0.020	0.70	0.61	0.09	0.014	0.53	0.46	0.07
Vienna	Max	0.036	0.73	0.60	0.13	0.014	0.53	0.47	0.06
	Mean	0.032	0.74	0.61	0.13	0.014	0.53	0.46	0.07
	Min	0.031	0.72	0.60	0.12	0.013	0.52	0.47	0.05
Zagreb-Gric	Mean	0.038	0.75	0.60	0.15	0.012	0.54	0.47	0.07
Rhein-Main	Min	0.020	0.70	0.61	0.09	0.010	0.52	0.48	0.04
Averaged variation		0.033	0.73	0.60	0.13	0.006	0.51	0.48	0.03

error, as mentioned above, the results shown in Table 2 indicate that the LTM variation signal seems to be significant. However, even so, we still need a more rigorous statistical significant test. From Table 2, we believe a more important result is that the averaged α variation (the gray thick line in Fig. 4) obtained from the temperature records maintains the statistical properties with larger standard deviation and variation range, while the result obtained from the shuffled data shows almost no variation due to the "average" procedure. This result is apparently associated with the variation patterns, as mentioned above. Variation of α arising from random statistical errors may be offset by the average procedure, while variations arising from intrinsic properties should not be affected. Therefore, to the end of this section, we take the averaged α variation (over 12 time series) as our research object, and make a statistical test.

To make the statistical test, we generate 120 000 artificial time series by using a autoregressive fractionally integrated moving average (ARFIMA) stochastic process (Caballero et al. 2002; Podobnik and Stanley 2008):

$$y_i \equiv \sum_{j=1}^{\infty} a_j(\rho) y_{i-j} + \eta_i, \tag{1}$$

where η_i denotes an independent and identically distributed (i.i.d.) Gaussian noise and $a_j(\rho)$ are statistical weights defined by

$$a_j(\rho) \equiv \frac{\Gamma(j-\rho)}{\Gamma(-\rho)\Gamma(1+j)}, \tag{2}$$

and $\Gamma(j)$ denotes the gamma function. Here ρ is a free parameter ranging from 0 to 0.5 and is related to the DFA exponent α as (Podobnik and Stanley 2008)

$$\alpha = 0.5 + \rho. \tag{3}$$

In this test, we use $\rho = 0.16$, which corresponds to the mean α value ($\alpha = 0.66$) of the 12 temperature records. The length of each artificial time series is 90 885, which corresponds to the length of 249-yr-long daily data (from 1763 to 2011). For each time series, we repeat our research procedures as introduced in section 2 and obtain an α variation by employing the sliding window analysis. To compare with the α variation averaged over 12 temperature records (the gray thick line in Fig. 4), we further average every 12 α variations obtained from the artificial data and finally get 10 000 (averaged) α variations. Based on these artificial α variations, we can determine the uncertainty intervals (owing to statistical errors) of the variation, and tell under what confidence

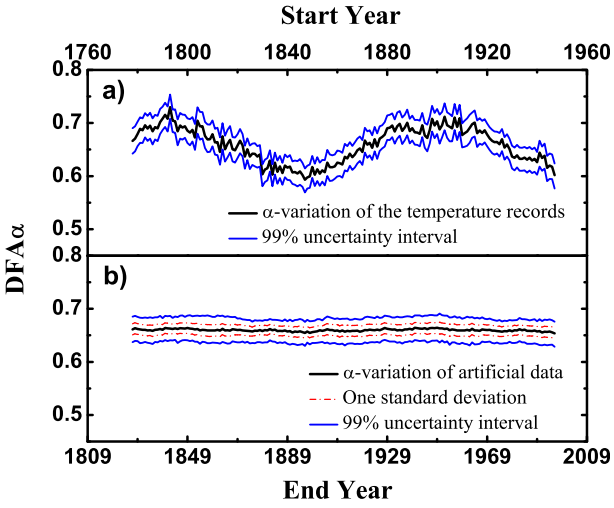

FIG. 5. Shown are α variations with uncertainty bounds: (a) the α variation of the temperature records (black curve), and (b) the results of the artificially generated data (black curve). The blue curves represent the uncertainty bounds of 99% confidence interval, while the red dashed line denotes the uncertainty bounds of one standard deviation. It is easy to find that there is no α variation in the artificial data, and the α variation obtained from the temperature records is significant, even after we take the uncertainty bounds into account. As in Figs. 3b and 4, numbers at the top (bottom) of the figure are the start year (end year) of each time window.

probability the α variations in the temperature records are significant. Figure 5 shows the results. From Fig. 5b, we can see that there is no α variation in the artificially generated data, which is as expected. After we take the uncertainty intervals (shown in Fig. 5a) into account, as shown in Fig. 5a, the α variation obtained from the temperature records is still remarkable. Therefore, we have reason to believe that the α variation obtained from the temperature records is indeed associated with the intrinsic properties of the time series, and the LTM does have a century-scale cycle signal.

We would like to note that the length of the sliding window, 50 yr, is not specific. With other choices, such as 40 or 60 yr (not shown here), one can still reach similar conclusions.

According to the previous discussion (Fig. 1), we know that the stronger the LTM is, the more apparent large-scale variability might be. Therefore, the century-scale variation cycle of LTM indicates a possible century-scale intensity modulation of the large-scale temperature variability. That is, at the beginning of the nineteenth and twentieth centuries, the large-scale variability is more apparent, whereas at the second half of the nineteenth and twentieth centuries the large-scale variability becomes less significant (see Fig. 4). How to understand this century-scale modulation is of great

importance and will be relevant for the research of climatic change, especially for a better climate prediction. The next section provides a brief discussion of this phenomenon.

4. Conclusions and discussion

In this study, we mainly focus on what the intensity (or significance) of the large-scale temperature variability may be like in different historical periods. We find that long memory analysis can be used to detect this possible intensity variation quantitatively. By determining the LTM of subrecords from different time intervals, one can see a century-scale variation of LTM. Although limited by the data length, such that we only discuss LTM on scales from 3 months up to 3 yr, the results can still further indicate a possible century-scale intensity modulation of the temperature variability. At the beginning of the nineteenth and twentieth centuries, the large-scale variability is more apparent, whereas at the second half of the nineteenth and twentieth centuries the large-scale variability becomes less significant.

To understand this phenomenon, more work and new mechanisms are needed. Recently, it has been recognized that nonstationarity can be one of the origins of the LTM (or the so-called long-range dependence), such as the persistent atmospheric regime behavior discussed by Franzke et al. (2011). The author suggests that jet stream regime behavior in the North Atlantic is a likely reason of the observed LTM (Franzke 2013). Therefore, changes of the regime behavior may cause oscillations and further can be used as a mechanism to explain the variation cycle of the LTM revealed in this study. However, it should be noted that even the variability of the atmospheric regime behavior itself is governed by more fundamental processes such as the North Atlantic Ocean variability, among others (Franzke et al. 2011; Franzke 2013). Therefore, considering that the time scales we are talking about in this study are large, we believe that the slow change effect of the Atlantic Ocean (Grosfeld et al. 2007; Zhang et al. 2007) should play an important role in interpreting this century-scale variation. In fact, as shown in previous studies (e.g., Blender and Fraedrich 2003), it is only when taking the oceanic variability into account, such as in a coupled atmosphere–ocean general circulation model (AOGCM), that one can possibly reproduce the LTM observed in instrumental records. Similarly, we believe the century-scale modulation of the temperature variability should also be attributed to the oceanic variability. For better understanding its mechanism, more detailed research combined with climate models is needed, such as a careful examination of whether the oceanic variability can drive a century-scale intensity modulation of the temperature variability.

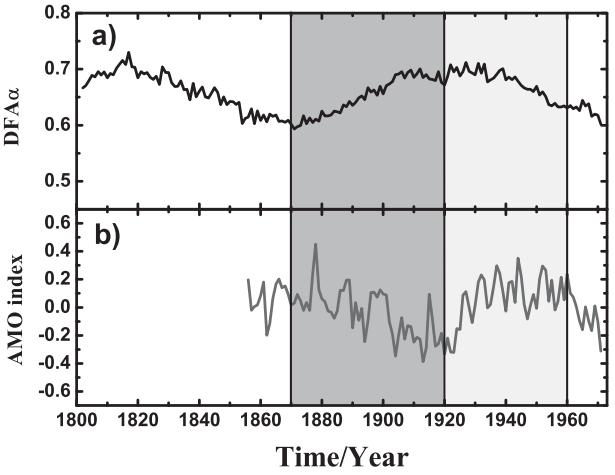

FIG. 6. Relationship between the (a) α variation and (b) AMO index. A close relationship between them is apparent. During the periods of 1870–1920 and 1920–60, increasing (decreasing) α corresponds to decreasing (increasing) AMO index. In the last 10 yr (1960–70), the opposite varying trends between them seem to disappear.

Here, a well-known mode of variability, the Atlantic multidecadal oscillation (AMO) (Schlesinger and Ramankutty 1994), should not be ignored. AMO represents a multidecadal oscillation occurring in the Atlantic Ocean and is normally defined from the patterns of SST variability in the North Atlantic. It has been recognized that AMO is closely related to the observed variations (such as the temperature, rainfall, etc.) over much of the Northern Hemisphere, especially in North America and Europe (Delworth and Mann 2000; Gray et al. 2004; Sutton and Hodson 2005). Therefore, it may also be a possible cause of the large-scale variation of the LTM (or the intensity modulation of the temperature variability) revealed in this study. In Fig. 6, we present the AMO index and the α variation (Fig. 4) together. The AMO index is available from the website of the National Oceanic and Atmospheric Administration (NOAA)'s Physical Science Division (PSD) Earth System Research Laboratory (ESRL) (http://www.esrl.noaa.gov/psd/data/climateindices/list/) and comprises annual data. Since we apply DFA to subrecords of 50 yr, the α obtained is thus mapped to the middle year. For example, if we apply DFA to the subrecord of 1901–50, the α value is mapped to the year of 1925. Limited by the sliding-window analysis as introduced in section 2, we only show the α variation from 1802 to 1971 (Fig. 6a), while the corresponding AMO index from 1856 to 1971 is also shown in Fig. 6b. Interestingly, a good relationship between them seems to exist. Especially during the

periods of 1870–1920 and 1920–60, increasing (decreasing) α corresponds to decreasing (increasing) AMO index. However, in the last 10 yr of data (1960–70), the opposite varying trends between them seem to disappear. Why does the LTM becomes stronger (weaker) when the AMO index is on a decreasing (increasing) trend during the period of 1870–1960? Why did the relationship change in the last 10 yr? Are there any mechanisms that can interpret the relationship between them? These questions are still unclear, and more detailed work is needed in the future.

Moreover, besides the oceanic variability, external forcing such as the solar activity (which is characterized by multidecadal variability; Lohmann et al. 2004; Soon 2005) should also be taken into account. We will give a detailed discussion on this research (combined with climate models) in a subsequent paper, but our findings herein are still interesting and show a new perspective on the research of climate change.

Acknowledgments. We thank three anonymous reviewers for their comments, which helped improve an earlier version of this manuscript. This study is funded by the National Natural Science Foundation of China (41175141) and the Basic Research Fund of CAMS (Grants 2013Z002).

REFERENCES

Becker, D. E., L. C. Peterson, J. T. Overpeck, A. Kaplan, M. N. Evans, and M. Kashgarian, 1999: Eight centuries of North Atlantic Ocean atmosphere variability. *Science,* **286,** 1709–1713.

Blender, R., and K. Fraedrich, 2003: Long time memory in global warming simulations. *Geophys. Res. Lett.,* **30,** 1769, doi:10.1029/2003GL017666.

Caballero, R., S. Jewson, and A. Brix, 2002: Long memory in surface air temperature: Detection, modeling and application to weather derivative valuation. *Climate Res.,* **21,** 127–140.

Chen, X., G. Lin, and Z. Fu, 2007: Long-range correlations in daily relative humidity fluctuations: A new index to characterize the climate regions over China. *Geophys. Res. Lett.,* **34,** L07804, doi:10.1029/2006GL027755.

Delworth, T. L., and M. E. Mann, 2000: Observed and simulated multidecadal variability in the Northern Hemisphere. *Climate Dyn.,* **16,** 661–676.

Dima, M., and G. Lohmann, 2004: Fundamental and derived modes of climate variability: Concept and application to interannual time-scales. *Tellus,* **56A,** 229–249.

Fraedrich, K. and R. Blender, 2003: Scaling of atmosphere and ocean temperature correlations in observations and climate models. *Phys. Rev. Lett.,* **90,** 108501, doi:10.1103/PhysRevLett.90.108501.

Franzke, C., 2013: Persistent regimes and extreme events of the North Atlantic atmospheric circulation. *Philos. Trans. Roy. Soc.,* **371A,** 20110471, doi:10.1098/rsta.2011.0471.

——, and T. Woollings, 2011: On the persistence and predictability properties of North Atlantic climate variability. *J. Climate,* **24,** 466–472.

——, ——, and O. Martius, 2011: Persistent circulation regimes and preferred regime transitions in the North Atlantic. *J. Atmos. Sci.,* **68,** 2809–2825.

Gray, S. T., L. J. Graumlich, J. L. Betancourt, and G. T. Pederson, 2004: A tree-ring based reconstruction of the Atlantic multidecadal oscillation since 1576 A.D. *Geophys. Res. Lett.,* **31,** L12205, doi:10.1029/2004GL019932.

Grosfeld, K., G. Lohmann, N. Rimbu, K. Fraedrich, and F. Lunkeit, 2007: Atmospheric multidecadal variations in the North Atlantic realm: Proxy data, observations, and atmospheric circulation model studies. *Climate Past,* **3,** 39–50.

Hasselmann, K., 1976: Stochastic climate models, Part I: Theory. *Tellus,* **28,** 473–485.

Kantelhardt, J. W., E. Koscielny-Bunde, H. H. A. Rego, S. Havlin, and A. Bunde, 2001: Detecting long-range correlations with detrended fluctuation analysis. *Physica A,* **295,** 441–454.

Keenlyside, N. S., M. Latif, J. Jungclaus, L. Kornblueh, and E. Roeckner, 2008: Advancing decadal-scale climate prediction in the North Atlantic sector. *Nature,* **453,** 84–88.

Koscielny-Bunde, E., A. Bunde, S. Havlin, H. E. Roman, Y. Goldreich, and H. J. Schellnhuber, 1998: Indication of a universal persistence law governing atmospheric variability. *Phys. Rev. Lett.,* **81,** 729–732.

Lennartz, S. and A. Bunde, 2009: Trend evaluation in records with long-term memory: Application to global warming. *Geophys. Res. Lett.,* **36,** L16706, doi:10.1029/2009GL039516.

Lohmann, G., N. Rimbu, and M. Dima, 2004: Climate signature of solar irradiance variations: Analysis of long-term instrumental, historical, and proxy data. *Int. J. Climatol.,* **24,** 1045–1056.

Mann, M. E., 2011: On long range dependence in global surface temperature series. *Climatic Change,* **107,** 267–276.

——, J. Park, and R. S. Bradley, 1995: Global interdecadal and century-scale climate oscillations during the past five centuries. *Nature,* **378,** 266–270.

——, R. S. Bradley, and M. K. Hughes, 1998: Global-scale temperature patterns and climate forcing over the past six centuries. *Nature,* **392,** 779–787.

Marshall, J., and Coauthors, 2001: North Atlantic climate variability: Phenomena, impacts and mechanisms. *Int. J. Climatol.,* **21,** 1863–1898.

Ottera, O. H., M. Bentsen, H. Drange, and L. Suo, 2010: External forcing as a metronome for Atlantic multidecadal variability. *Nat. Geosci.,* **3,** 688–694.

Peng, C. K., S. V. Buldyrev, S. Havlin, M. Simons, H. E. Stanley, and A. L. Goldberger, 1994: Mosaic organization of DNA nucleotides. *Phys. Rev.,* **49E,** 1685–1689.

Podobnik, B. and H. E. Stanley, 2008: Detrended cross-correlation analysis: A new method for analyzing two nonstationary time series. *Phys. Rev. Lett.,* **100,** 084102, doi:10.1103/PhysRevLett.100.084102.

Rybski, D., and A. Bunde, 2009: On the detection of trends in long-term correlated records. *Physica A,* **388,** 1687–1695.

——, ——, S. Havlin, and H. von Storch, 2006: Long-term persistence in climate and the detection problem. *Geophys. Res. Lett.,* **33,** L06718, doi:10.1029/2005GL025591.

Schlesinger, M. E., and N. Ramankutty, 1994: An oscillation in the global climate system of period 65–70 years. *Nature,* **367,** 723–726.

Soon, W. W. H., 2005: Variable solar irradiance as a plausible agent for multidecadal variations in the Arctic-wide surface air temperature record of the past 130 years. *Geophys. Res. Lett.,* **32,** L16712, doi:10.1029/2005GL023429.

Sutton, R. T., and D. L. R. Hodson, 2005: Atlantic Ocean forcing of North American and European summer climate. *Science,* **309,** 115–118.

Talkner, P., and R. O. Weber, 2000: Power spectrum and detrended fluctuation analysis: Application to daily temperatures. *Phys. Rev.,* **62E,** 150–160.

Vyushin, D. I., and P. J. Kushner, 2008: Power-law and long-memory characteristics of the atmospheric general circulation. *J. Climate,* **22,** 2890–2904.

Zhang, R., T. L. Delworth, and I. M. Held, 2007: Can the Atlantic Ocean drive the observed multidecadal variability in Northern Hemisphere mean temperature? *Geophys. Res. Lett.,* **34,** L02709, doi:10.1029/2006GL028683.

Zhu, X., K. Fraedrich, Z. Liu, and R. Blender, 2010: A demonstration of long-term memory and climate predictability. *J. Climate,* **23,** 5021–5029.